A Computational Method of Investigating Natural Substances from *Cyperus rotundus* L. as Potential Brown Planthopper *Nilaparvata lugens* (Stål) Acetylcholinesterase Inhibitors

Saqib Hussain Bangash[1,2], Chen-Yang Wei[1], Akbar Ali[3], Muhammad Ibrahim[2], Fan-Dan Li[1], Amjad Hussain[4], and Wen-Wei Tang[1*]

[1]*Guangxi Key Laboratory of Agri-Environment and Agric-Product Safety, College of Agriculture, Department of Crop Environment and Ecology, Guangxi University, Nanning 530004, China*

[2]*Department of Applied Chemistry, Government College University, Faisalabad 38000, Pakistan*

[3]*Department of Chemistry, Government College University, Faisalabad 38000, Pakistan*

[4]*Institute of Chemistry, University of Okara, Okara-56300, Punjab, Pakistan*

* ***Corresponding author:***

email: wenweitg@163.com

Received: March 22, 2025
Accepted: July 31, 2025

DOI: 10.22146/ijc.105603

Abstract: *Brown rice planthopper (*Nilaparvata lugens *(Stål)) is a highly damaging pest of rice that has led to considerable losses in yields, increasing resistance to most conventional insecticides demands the adoption of eco-friendly chemical solutions.* Cyperus rotundus *L., a medicinal plant unaffected by* N. lugens *and reported to possess insecticidal properties, was selected for its potential to inhibit acetylcholinesterase (AChE), a key insect nervous system enzyme. Nine phytochemicals isolated from* C. rotundus *were evaluated through molecular docking, with quercetin (−8.9 kcal/mol), biochanin A (−8.7 kcal/mol), and cyperotundol (−8.1 kcal/mol) outperforming the positive control, carbofuran (−8.2 kcal/mol). The identified phytochemicals proved to have better binding affinity and complex stability, evidenced by the reduced values of RMSD/RMSF and more lasting interactions over 100 ns MD simulations compared to the positive control in both domain movement and binding stability. MMGBSA estimated favorable binding free energies (−67.06, −57.11, −71.07 kcal/mol) versus carbofuran (−36.84 kcal/mol). These findings suggest that* C. rotundus *phytochemicals are promising natural AChE inhibitors and potential candidates for sustainable* N. lugens *control. Their effectiveness implies the eco-friendly use of these natural compounds as a possible factor in the use of fewer and non-synthetic insecticides in pest control or integrated pest management.*

Keywords: *brown planthopper; acetylcholinesterase; molecular docking; molecular dynamics*

■ INTRODUCTION

Rice (*Oryza sativa*) is a vital staple crop globally, particularly in Asia and the Pacific, providing essential calories and significant economic value to millions of people [1]. Yet, rice cultivation faces multifaceted, biotic and abiotic challenges as it strives to meet escalating consumption demands. Among these, insect pests present one of the most formidable threats, frequently causing plant wilting and serving as vectors for various pathogens. Notably, the brown planthopper (*Nilaparvata lugens* (Stål)), BPH) is one of the most destructive pests of rice, severely curtailing yields across major rice-producing nations and causing the notorious "hopper burn" [2]. By inserting its stylet to feed on phloem sap, BPH inflicts mechanical damage, depletes vital nutrients and water, and transmits multiple viruses, such as the rice ragged stunt virus [3-4]. Thus, the predominant strategy has relied on chemical insecticides [5].

Intensive and continual pesticide use has driven the evolution of profound resistance in BPH, notably to

phenylpyrazoles (flufiprole, ethiprole), carbamates (isoprocarb), pyridine azomethine derivatives (pymetrozine), chitin biosynthesis inhibitors (buprofezin), and neonicotinoids (imidacloprid, thiamethoxam, clothianidin, dinotefuran) [6]. According to the Arthropod Pesticide Resistance Database (APRD), 456 resistance cases spanning 36 pesticide active ingredients have been recorded worldwide for BPH [7]. In Asia, neonicotinoids remain the primary pesticide class employed for BPH control [8]. Yet, decade-long surveillance reveals that BPH has developed high resistance levels against key neonicotinoids, including thiamethoxam, clothianidin, imidacloprid, and dinotefuran, especially in China [9]. In response, Takeda Agro introduced nitenpyram (NIT)—a second-generation neonicotinoid—in 1995, later commercialized in China in 2007 [10]. Though BPH resistance to NIT has increased with continued use, current resistance remains moderate ($10.0 \leq$ resistance ratio < 100.0) [11-12], allowing it to retain as a primary management tool. Nevertheless, compared to longer-lasting insecticides like imidacloprid, NIT's short environmental persistence and declining efficacy within 5 days post-application necessitate multiple applications per season. This repeated use accelerates resistance development and exacerbates environmental contamination [10,13].

Acetylcholine esterase (AChE) is a neurotransmitter-hydrolyzing enzyme essential to neural signal termination. Altered AChE activity is a principal resistance mechanism in numerous insect pests, commonly documented in carbamate- and organophosphate-resistant species [14]. AChE can be irreversibly inhibited by phosphorylating its active-site serine hydroxyl group with organophosphates [15-16]. Beyond synthetic compounds, natural products like neem (*Azadirachta indica*) extracts also impair AChE activity—for instance, Vepacide (a neem seed oil derivative) significantly reduced AChE activity in rat brains at 80, 160, and 320 mg/kg [17].

Recently, we explored the bioactive potential of *Cyperus rotundus* L., revealing its capacity to isolate new natural compounds with insecticidal and enzyme-inhibitory activities. Phytochemical analyses identified molecules with potent inhibitory effects on AChE and glutathione S-transferase—crucial enzymes for insect neural transmission and detoxification. Notably, these compounds demonstrated remarkable insecticidal activity against *N. lugens*, positioning *C. rotundus* as a promising eco-friendly biopesticide source [18]. Conventional drug discovery methods, though foundational, are notoriously laborious, protracted (typically spanning 10–15 years), and financially demanding [19-20]. Dishearteningly, these traditional approaches suffer from low success rates and high attrition, with absorption, distribution, metabolism, excretion, and toxicity (ADME) shortcomings accounting for nearly half of all late-stage failures [21-22]. In contrast, computer-aided drug discovery and development has revolutionized the field, substantially reducing timelines and costs by leveraging computational power [23]. Computer-aided drug design, particularly modeling and docking, offers a viable, efficient alternative to streamline discovery pipelines [24].

The integration of molecular simulations, including molecular docking and molecular dynamics simulations (MD), has become indispensable in elucidating protein structure-function relationships [25]. Virtual screening and MD facilitate the prediction of molecular docking affinities, biological system simulations, and dynamics analyses of protein-ligand interactions [26]. These strategies offer superior accuracy in drug development, revealing binding modes and informing the rational design of highly effective inhibitors [27]. Simplified scoring functions, emphasizing hydrophobic interactions and hydrogen bonds (H-bonds) while often neglecting entropy, are typically used to expedite computations by minimizing degrees of freedom. Consequently, this study seeks to validate computational predictions with supporting *in vitro* assays to strengthen the reliability of our findings [28-29]. This study aims to identify and evaluate natural compounds from *C. rotundus* for anti-BPH activity via AChE inhibition. We employed molecular docking, MD simulation, and the molecular mechanics generalized Born surface area (MMGBSA) method to calculate binding free energies. Although various scoring schemes

exist for estimating protein-ligand interaction energies, current methodologies struggle to reliably predict native binding modes and precise free energy values due to the inherent trade-offs between computational efficiency and predictive accuracy.

■ COMPUTATIONAL SECTION

Materials

The AChE protein, having accession number AF-G9BJC1-F1, was retrieved from the AlphaFold database (http://www.AlphaFold.org). AlphaFold is the first computational technique based on a neural network model, capable of accurately predicting protein structures even in the absence of homologous templates, achieving very high confidence scores (> 90% pLDDT). Following an extensive literature review, 9 compounds were selected for further investigation. Their structures (Fig. 1) were retrieved from the PubChem database [30] and ChemSpider [31]. To ensure the accuracy and reliability of the results, molecular docking was first conducted to predict the ligands' binding affinities and interaction profiles with the target protein. The top-ranked complexes were then subjected to MD simulations to evaluate the stability and dynamic behavior of the protein-ligand interactions over time. Finally, MMGBSA binding free energy calculations were performed on the MD-refined complexes to better estimate binding energies.

Instrumentation

AutoDock Vina was employed to generate all potential binding geometries based on its scoring function, which estimates binding affinity by evaluating factors such as van der Waals interactions, H bond, electrostatics, and desolvation energies. This approach facilitates the identification of optimal ligand conformations within the active site of target proteins [32-33]. PROCHECK (v3.5; European Bioinformatics Institute, UK), ERRAT (UCLA, USA), and Verify3D (Structural Analysis and Verification Server, UCLA, USA) were utilized for the stereochemical validation of the modeled protein structures [34-35]. The SwissADME online tool (Swiss Institute of Bioinformatics, Lausanne, Switzerland) was applied to assess drug-likeness and pharmacokinetic properties [36]. The protein-ligand interactions were visualized using UCSF Chimera [37] and Discovery Studio Visualizer [38]. Desmond v6.5 (Schrödinger LLC, New York, NY, USA) was used for MD simulations [39]. Maestro 2019.1 (Schrödinger LLC, New York, NY, USA) was used for protein-ligand preparation and system building [40]. The Prime MMGBSA module (Schrödinger LLC, New York, NY, USA) was utilized for binding free energy (ΔG_{bind}) calculations during MD simulations.

Procedure

Protein preparation

Polar hydrogen atoms were added to the protein and ligand structures using AutoDockTools. Subsequently, Gasteiger charges were computed, and non-polar hydrogens were merged. The prepared structures

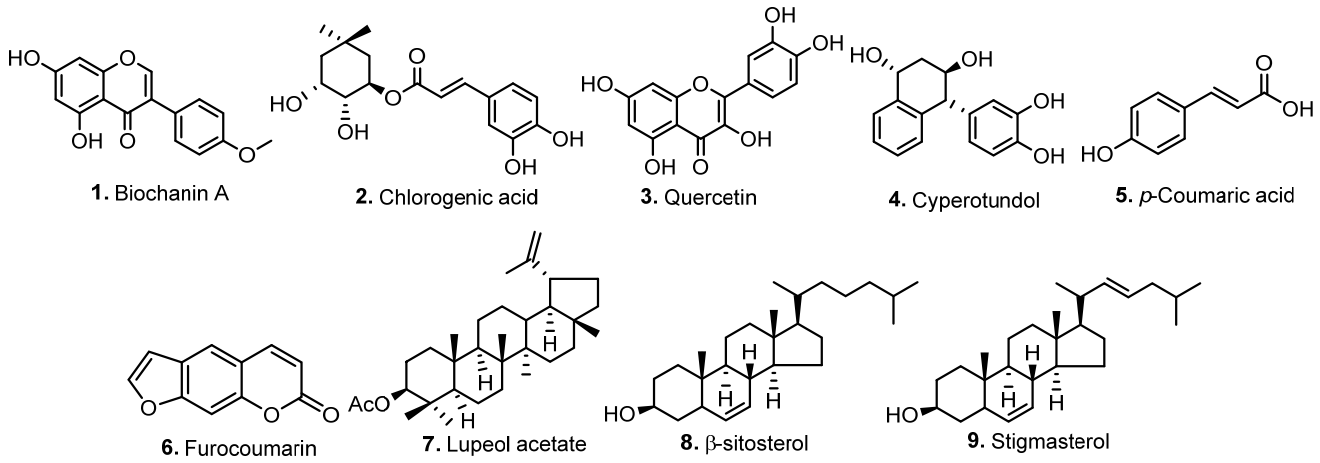

Fig 1. Structure of the 9 compounds used as natural inhibitors

were then saved in PDBQT format, which is required for AutoDock Vina [32].

Preparation of ligands

The isolated compounds were first converted into MOL2 format using Open Babel. Energy minimization was then performed using the MMFF94 force field within Open Babel to optimize the geometry of the compounds. The minimized structures were subsequently processed using AutoDock Tools, where polar hydrogen atoms were added, Gasteiger charges were computed, torsion flexibility was defined, and the ligands were saved in PDBQT format for molecular docking analysis [41].

Validation of the modeled structures

The 3D predicted structures of the target protein were validated using PROCHECK, ERRAT, and Verify3D tools accessed through the online server (https://saves.mbi.ucla.edu/). PROCHECK generated the Ramachandran plot illustrating favorable and unfavorable residue regions, ERRAT analyzed non-bonded atomic interactions using a sliding window approach, and Verify3D assessed the compatibility between the 3D model and the amino acid sequence based on secondary structure elements such as helices, sheets, and loops [42-43].

Drug-likeness and ADME studies

Lipinski's Rule of Five was applied to assess the drug-likeness of the screened compounds, ensuring their potential to interact with target proteins or enzymes [44]. Pharmacokinetics properties and drug metabolism were also evaluated, acknowledging the high failure rate often observed during clinical trials [22]. The SwissADME tool was used to predict ADME characteristics of the screened compounds [36].

Molecular docking analyses

AutoDock Vina was utilized to generate all potential binding geometries based on its scoring function. It estimates binding affinity by evaluating van der Waals interactions, H-bond, electrostatics, and desolvation energies. This approach facilitates the identification of optimal ligand conformations within the active site of target proteins [32,45]. The estimated binding energy (ΔG) was calculated using AutoDock's scoring function, which accounts for van der Waals forces, electrostatic interactions, H-bonds, torsional entropy, and desolvation effects to predict ligand binding affinity. Molecular docking investigates the interactions between the isolated compounds and the active site of BPH AChE. The binding affinities were estimated using the Generalized Born Volume Integral/Weighted Surface Area (GBVI/WSA dG) scoring function, a force field-based method that calculates the free energy of binding by incorporating solvation effects and molecular mechanics energies. This approach has been demonstrated to effectively predict ligand binding modes and affinities in various protein-ligand systems [46].

MD simulation

MD simulations were performed using the Desmond software [47] for 100 ns. Rigid binding assessments of the selected compounds against the target protein were determined through MD simulations [48]. Newton's classical equations of motion were applied to model ligand behavior under physiological conditions [49-50]. Proteins and ligands were optimized using Maestro's Protein Preparation Wizard. At the same time, the simulation system was constructed using the System Builder tool with an orthorhombic box and the OPLS_2005 force field, along with the TIP3P water model [51]. Simulation conditions included a temperature of 300 K, a pressure of 1 atm, and 0.15 M NaCl. Counterions were added to neutralize the system. Trajectory frames were recorded every 100 ps, and root mean square deviation (RMSD) analyses were conducted to monitor the structural stability of the protein-ligand complexes [52-53].

MMGBSA calculations

The binding free energy (ΔG_{bind}) of docked complexes during MD simulations was estimated using the MMGBSA approach within the Prime module. Calculations were performed using the OPLS_2005 force field, the VSGB solvation model, and a rotamer search technique using Eq. (1) [54];

$$\Delta G_{bind} = \Delta G_{complex} - \left(\Delta G_{protein} + \Delta_{Gligand}\right) \quad (1)$$

where, ΔG_{bind} = binding free energy, $\Delta G_{complex}$ = free energy of the complex, $\Delta G_{protein}$ = free energy of the target protein, and ΔG_{ligand} = free energy of the ligand.

Protein-ligand interaction

The Protein-Ligand Interaction Profiler (PLIP; https://plip-tool.biotec.tu-dresden.de) was used to analyze and map the interactions between the target protein and the three ligands exhibiting the highest binding affinities, along with the positive control, to identify similarities in the interacting residues. The PLIP is a widely recognized for analyzing non-covalent interactions between proteins and ligands. The 2021 update of PLIP expanded its capabilities to include interactions with DNA and RNA, enhancing its utility in structural bioinformatics and drug discovery. This version provides detailed insights into various interaction types, such as H-bonds, hydrophobic contacts, π-stacking, π-cation interactions, salt bridges, water bridges, metal complexes, and halogen bonds. PLIP offers a web interface and command-line tools, facilitating integration into high-throughput computational pipelines. The tool has been instrumental in characterizing docking experiments and assessing novel ligand–protein complexes, making it a valuable resource in the development of insecticides and other therapeutic agents [55]. The resulting interactions were further visualized and analyzed using UCSF Chimera and Discovery Studio.

■ RESULTS AND DISCUSSION

The 3D structure of the target protein AChE with accession number AF-G9BJC1-F1, Structural model obtained from AlphaFold database [56]. For further analyses, the missing residues within the designated protein structure were anticipated, refined, and reduced. The target protein's loop was refined, enough hydrogen atoms were added, and the right bond order was assigned to obtain the protein's native conformation [57-58]. Different stereochemical parameters of the protein structure, such as PROCHECK, ERRAT, and Verify3D, were utilized to assess the efficacy of the predicted model, and the model with the highest accuracy was selected for further analysis (Fig. 2).

PROCHECK analyzes the overall model geometry by generating the Ramachandran plot with favorable and non-favorable residue regions, in which the red, yellow, and black colors, respectively, denote the most favorable, favorable, and disallowed region; the torsion angle,

Fig 2. The 3D predicted structure of BPH AChE protein (*N. lugens*)

represented by the Phi and Psi bonds, predicts the potential shape of the peptides, as shown in Fig. 3(a). The ERRAT, a database of highly refined protein structures with nine sliding windows of residue vs error. Verify3D validates a 3D structure in terms of loops, sheets, and alpha helices [59-60]. In Fig. 3(b), ** is expressed as the proportion of the protein for which the estimated error value falls below the 95% rejection level; two lines are placed on the error axis to represent the confidence with which it is possible to reject sections that exceed that error value. Typically, well-designed high-resolution structures yield values of approximately 95% or more. The overall quality factor is at a lower degree of 2.5 to 3.0 Å, 91%. The confidence levels of 95% and 99% are shown by the yellow and red bars, respectively. The Ramachandran plots for AChE are shown in A. In ERRAT, AChE structures show an overall quality factor of 92.53. In the Verify3D model verification, where the minimum passing score was 80%, the 3D models received 84.74% (Fig. 3(c)). The ProSA-web server was utilized to compare the protein structural models to the PDB's protein structures based on the Z-score [61] (Fig. 3(d)).

Molecular Docking Analysis

AChEs exhibit point mutations that make resistance to carbamates and organophosphates; insecticide resistance is often the consequence of target site insensitivity in *N. lugens* [62]. AChE in insects has

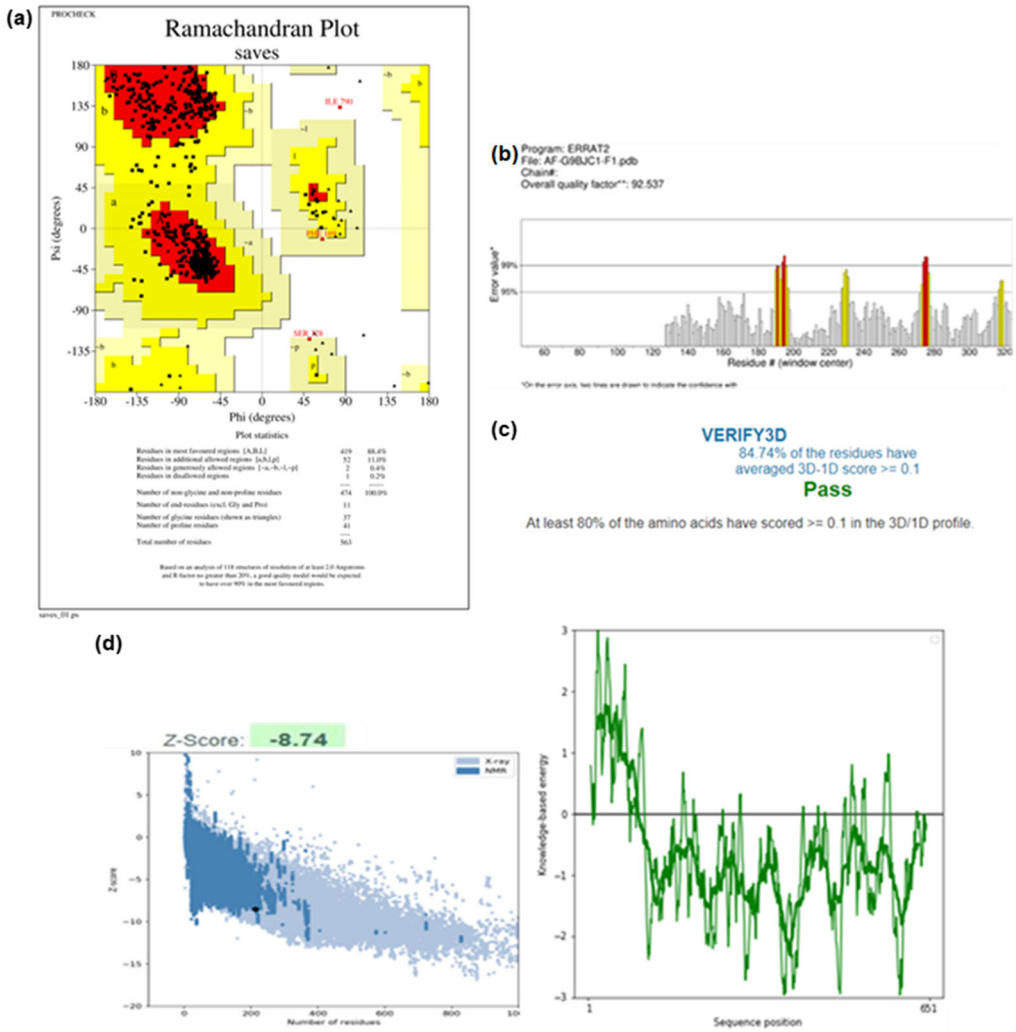

Fig 3. The 3D structure of brown planthopper (*N. lugens*) acetylcholinesterase (AChE) was confirmed using (a) the Ramachandran plot generated by PROCHECK, (b) the server quality factor (ERRAT), (c) Verify3D, and (d) ProSA-web (Z-score)

been suggested as the primary catalytic enzyme due to its high expression level and frequent point mutations linked to pesticide resistance [63]. Therefore, molecular docking research was conducted to determine the molecular interactions between the target protein and nine selected ligands isolated from *C. rotundus*. The aim was to use AChE as the primary target for developing new insecticides. Using the AutoDock Vina tool, these phytochemicals were docked with the active AChE site.

Three compounds were selected based on less binding energy than the reference control pesticide carbofuran and have a propensity to interact and disrupt the function of AChEs (Table 1). The ligands with higher binding energies were determined to be quercetin, biochanin A, and cyperotundol, which had binding energies of −8.9, −8.7, and −8.1 kcal/mol, respectively (Table 1). These ligands were then utilized to examine molecular interactions and pharmacokinetic parameters (Fig. S1). Strong insecticidal properties are displayed by quercetin, while chlorogenic acid has an antagonistic impact on quercetin. Quercetin's binding energy value was lower than that of chlorpyrifos in the molecular docking analyses conducted on the active site of *Spodoptera frugiperda* AChE. Furthermore, the interactions profile revealed π–π interactions between quercetin and the active sites [64].

Table 1. Binding affinities of ligands with AChEs of *N. lugens*

Ligands	Binding energy (kcal/mol)
Carbofuran (control)	−8.2
Biochanin A	−8.7
Cyperotundol	−8.1
p-Coumaric acid	−6.5
Chlorogenic acid	−7.7
Quercetin	−8.9
Furocoumarin	−7.8
Lupeol acetate	−6.7
β-sitosterol	−5.0
Stigmasterol	−2.6

Protein-Ligand Interaction

H-bonds are critical for the stabilization of ligand-AChE and complexes and contribute significantly to inhibitory potency. Recent studies have shown that H-bonds not only enhances the binding affinity but also improves selectivity towards insect AChEs. For example, Kukreja et al. [65] reported that H-bonds between natural inhibitors and key active site residues of *Helicoverpa armigera* AChE increased both affinity and insecticidal efficacy. Previous works also demonstrated that H-bonds in flavonoid-based inhibitors improved stability and inhibition efficiency against *S. frugiperda* AChE [66-67]. Hydrophobic contacts are equally important for anchoring inhibitors within the AChE binding pocket. These kinds of interactions with residues such as Trp and Phe significantly increased the potency of chalcones as AChE inhibitors for pest control [68]. The research confirmed that hydrophobic interactions contribute to inhibitor selectivity by fitting the unique hydrophobic pockets present in insect AChEs but absent in non-target organisms [69].

Using the PLIP tool, the molecular interactions between the ligands and receptor were analyzed. In addition to hydrophobic interactions, H-bond was the primary mechanism for chemical binding in the AChE's active site. A thorough analysis of the binding orientations of the top three phytochemical analogs, quercetin, biochanin A, and cyperotundol was conducted (Fig. S1). The best possible conformations were retrieved, which provided a detailed description of the amino acid residues involved in the interaction. H-bonds are the most prevalent directed intermolecular interactions in biological complexes [70]. These residues interact with ligands in four different ways: as hydrogen donors, hydrogen acceptors, Hydrophobic interactions, and in pi-pi interactions [71]. The intermolecular interactions observed to optimize ligand-receptor complexes can be utilized to synthesize entirely new molecules capable of interacting and inhibiting the target, with *in vitro* and *in vivo* biological activity [72].

Among all the phytocompounds, quercetin shows the strongest interaction of −8.9 kcal/mol with the AChE of the brown plant hopper *N. lugens*. H-bonds are the most prevalent type of directed inter molecular interactions in biological complexes The quercetin formed H bonds with five specific amino acids of the AChE Asp201, Tyr259, Tyr259, Tyr457, and His568, whereas Asp201, Trp213, Trp213, and Trp213, are involved in hydrophobic interactions (Table 2). The second-best compound revealed from the molecular docking analysis was biochanin A, with binding energy of −8.7 kcal/mol by interacting with the key amino acid residues, Asp201, Trp213, Gly247, and Ser251, this molecule fits into the receptor's active binding site stably. These residues are important for H-bonding, while Ile199, Asp201, and Tyr461 are involved in hydrophobic interaction (Table 2).

The binding energy between cyperotundol and AChE was measured at −8.1 kcal/mol. Six H-bonds and six hydrophobic interactions were also found between cyperotundol and AChE. The observed H-bonds with amino acids Gly246, Gly247, Gly248, Tyr259, Ser328, and Ser328, respectively. Hydrophobic interactions of cyperotundol and AChEs of *N. lugens* were also found with amino acid Trp213, Trp213, Trp213, Leu256, Tyr457, and Phe458 (Table 2). The interactions between the three ligands with minimum binding energies and the target protein were compared to the positive control carbofuran. It was observed that the three ligands bound at a similar pocket of the target protein and shared more than 80% of the binding site residues (Table 2).

Table 2. Molecular interactions of the best ligands against AchE of *N. lugens*

Ligands	Binding affinity (kcal/mol)	Interacting amino acids	
		Hydrogen bonds	Hydrophobic interactions
Carbofuran (positive control)	−8.2	Tyr250 (2.94 Å), Ser251 (2.09 Å), Gly247 (2.22 Å), Tyr259 (2.45 Å), Asp201 (2.54 Å)	Trp213 (3.64 Å), Asp201 (3.33 Å), Trp213 (3.12 Å)
Quercetin	−8.9	Asp201 (2.44Å), Tyr259 (2.33 Å), Tyr259 (2.81Å), Tyr457 (2.56 Å), His568 (2.40 Å)	Asp201 (3.91 Å), Trp213 (3.60 Å), Trp213 (3.01 Å), Trp213 (3.61 Å)
Biochanin A	−8.7	Asp201 (3.33 Å), Trp213 (2.27 Å), Gly247 (3.30Å), Ser251 (2.80 Å)	Ile199 (3.59Å), Asp201 (3.37 Å), Tyr461 (3.74 Å)
Cyperotundol	−8.1	Gly246 (2.75Å), Gly247 (2.97Å), Gly248 (2.82Å), Tyr259 (2.81Å), Ser328 (2.37Å), Ser328 (2.31Å)	Trp213 (3.48 Å), Trp213 (3.39 Å), Trp213 (3.61 Å), Leu256 (3.97 Å), Tyr457 (3.42 Å), Phe458 (3.63 Å)

Pharmacodynamic Analysis

Swiss ADME and Lipinski rule of five were utilized to assess the drug likeness of the screened compounds [73]. The number of rotatable bonds, H-bond donors, and acceptors was also calculated, including the drug-like properties of all the selected compounds, to assess the toxic behavior of the compounds. The Lipinski's rule of five was also calculated for all the selected compounds. The properties of ADME play a significant role in studying the distribution and absorption behavior of the compound in an organism. As per Lipinski's rule of five, the screened compound should not violate > 1 of the following conditions: the molecular weight of the compound should not > 500, the log P value should not > 5, H-bond acceptors should not > 10, and H-bond donors should not > 5.

For the ADME and drug-likeness analysis, Lipinski's rule of five was applied, where acceptable thresholds included a molecular weight ≤ 500 Da, log P ≤ 5, no more than 5 H-bond donors, and no more than 10 H-bond acceptors. Compounds violating more than one of these parameters were considered less drug-like. The topological polar surface area (TPSA) was also evaluated, with an ideal threshold of ≤ 140 $Å^2$ to ensure good membrane permeability. Compounds were also assessed for solubility (log S) and the number of rotatable bonds (≤ 10), which influence absorption and bioavailability. These thresholds align with established criteria for oral bioavailability and pharmacokinetic stability in bioactive compounds used for insecticide development and drug discovery [36,74].

Other relevant markers of high bioavailability, i.e., log P and TPSA values [75-76], were also examined, and it was observed that they varied from ~124.29 for TPSA and between 0.72 and 4.83 for log P. Lipophilicity, represented as log P, less than 5, indicates the substance's capacity for penetration of biological membranes [77]. On the other hand, it was observed that TPSA—which is the total of polar surfaces with atoms of oxygen, nitrogen, and hydrogen—is connected to a compound's H-bond capability [78]. Since a TPSA score of fewer than 140 $Å^2$ is desirable for drug-like molecules, it was observed that all the screened compounds fell between 20.23 and 124.29. Additionally, no compound violated Lipinski's rule of five by having a molecular weight less than 500. Increased bulkiness of the molecule is indicated by a higher molecular weight, which eventually impacts permeability [79]. Additionally, it is permitted to deviate from Lipinski's rule in two or fewer parameters [80]. Furthermore, the number of rotatable bonds was examined and determined to be ≤ 10 for every phytochemical, indicating that compounds can interact with the rigid protein's binding site [74] (Table 3).

MD Simulation

MD simulation analyses of the three selected protein ligand complexes, along with the positive control, were performed for 100 ns to analyze the radius of gyration (Rg), H-bonds, RMSD, and root mean square

Table 3. Drug-like properties of ligands

Name of ligands	MW (g/mol)	#H-bond acceptors	#H-bond donors	TPSA (Å²)	i log P	ESOL log S	Lipinski violations	Lead likeness violations
Biochanin A	284.26	5	2	79.90	2.55	-3.92	0	0
Cyperotundol	272.30	4	4	80.92	1.89	-2.91	0	0
p-Coumaric acid	163.15	3	1	60.36	0.97	-2.01	0	1 violation: MW < 250
Chlorogenic acid	322.35	6	4	107.22	1.46	-3.03	0	0
Quercetin	302.24	7	4	124.29	0.72	-3.22	0	0
Furocoumarin	186.16	3	0	43.35	2.01	-2.73	0	1 violation: MW < 250
Lupeol acetate	468.75	2	0	26.30	4.89	-9.13	1 violation: M log P > 4.15	2 violations: MW > 350, X log P3 > 3.5
β-Sitosterol	386.65	1	1	20.23	4.83	-7.41	1 violation: M log P > 4.15	2 violations: MW > 350, X log P3 > 3.5
Stigmasterol	384.64	1	1	20.23	4.76	-6.93	1 violation: M log P > 4.15	2 violations: MW > 350, X log P3 > 3.5

fluctuation (RMSF) to assess the compounds' stability. The relatively lower RMSD values compared to the positive control reflect the ligands' stability and binding consistency. After analyzing the RMSD plot of the compound quercetin with the target protein, it was observed that a smaller number of deviations were observed in the protein structure as the structure started deviating from 0.4 to 2.8 Å for the first 20 ns of the simulation time. The protein structure adapts to stability after the first 20 ns of the simulation time. The ligand quercetin was found to be deviating during the initial simulation period, but it became stable after 27 ns. Although minor deviations were observed in the ligand from 60 to 70 ns, those deviations were within the acceptable window of 1.5 Å overall. Overall, the protein ligand complex was found to be stable after initial 70 ns of the simulation time as the deviations were within the window of 3 Å suggesting that the protein did not suffer any structural change (Fig. 4(a)) According to the RMSF, it was observed that a fluctuation of 4.8 Å occurred from residue no 80 to 100. The overall protein was stable, although minor fluctuations were observed, confirming the target protein's flexibility (Fig. 4(b)). The average RMSF was 1.11 Å. This calculation revealed some variation, indicating a kinetic shift from the starting point.

The RMSD plot of biochanin A and the target protein complex revealed that the protein deviated from its initial position at the start of the simulation. After the initial 5 ns, the protein reached its equilibrium state. The average RMSD of the target protein was 2 Å; minor deviations were observed, indicating the flexibility of the protein structure. On the other hand, the compound Biochenin A was also found to be stable during the first 60 ns of the simulation period. A deviation was observed from 1.5 to 3.5 Å in the ligand after 60 ns, but the ligand became stable after 70 ns. Overall, the protein ligand complex was found to be stable in case of biochenin A as the average RMSD between the ligand and the target protein was almost 1.5 A which is within the acceptable window (Fig. 4(c)). The RMSF analysis of the target protein was also found to be stable as the binding pocket regions was observed to be stable with some minor fluctuations indicating the flexibility of the protein binding pocket. The average RMSF calculated was 1.11 Å (Fig. 4(d)).

According to the RMSD analyses of the cyperotundol and the target protein, it was observed that the target protein was found to be stable throughout the simulation time. Although minor deviations were observed in the protein structure, the protein slightly deviated at 40 ns from 2.8 to 1.6 Å. After 40 ns, the protein was stable throughout the simulation time. During the simulation period, the ligand cyperotundol was found to be deviating during the initial timeframe as the ligand deviated from 1.2 to 5.2 Å from 10 to 18 ns, respectively. Minor deviations were observed in the ligand throughout the simulation time. Still, the ligand got stable during the final stages as the RMSD recorded was 3.5 Å, which is within the acceptable window. According to the RMSD analyses, the protein ligand complex was found to be stable as the RMSD recorded between the protein and the selected ligand was less than 1 Å (Fig. 4(e)). According to the RMSF analysis, the protein was found to be stable throughout the simulation time. Fluctuations were observed between the 40–100 and 310–380 residue region was found to be fluctuating, but the binding site regions were found to be

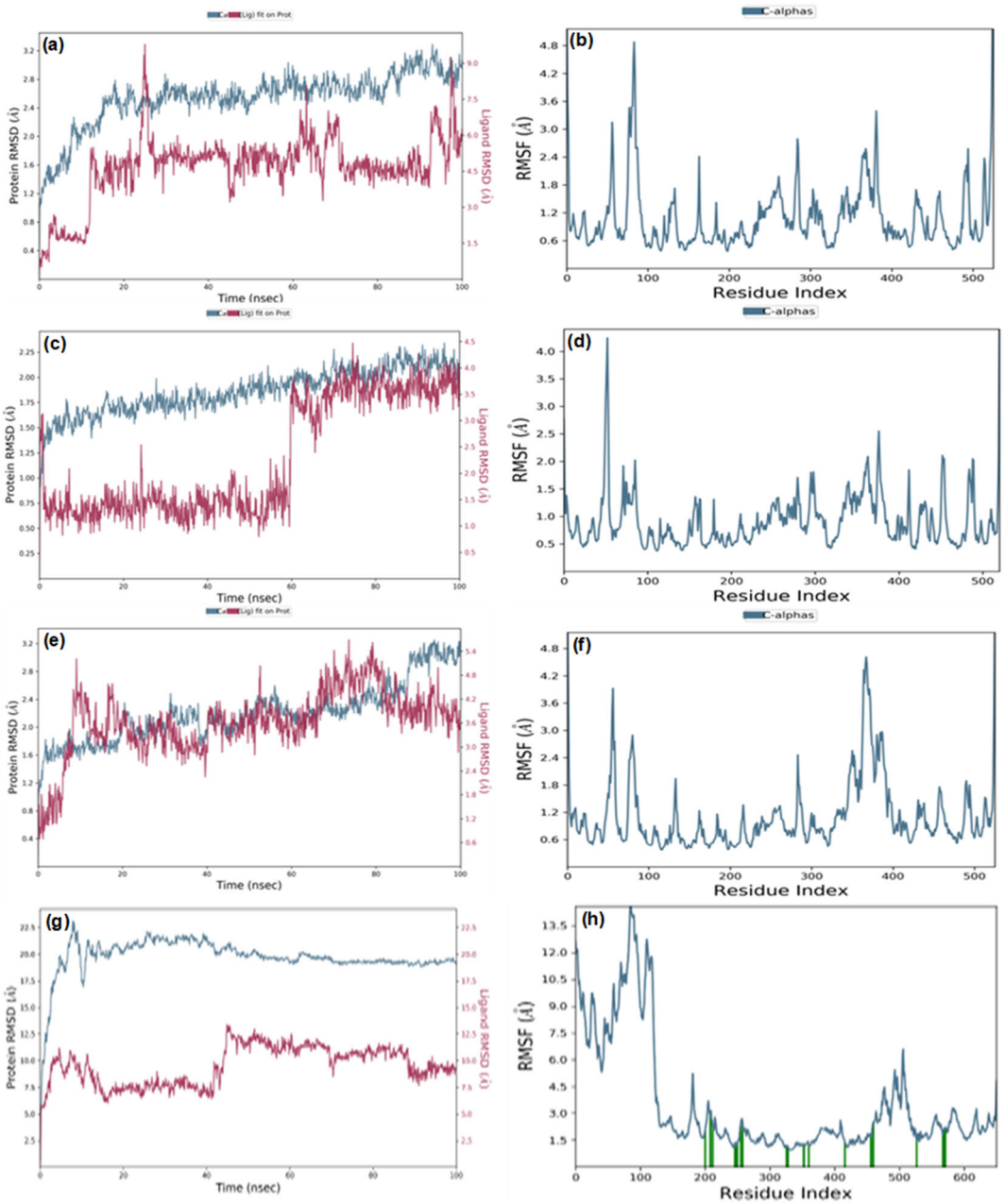

Fig 4. RMSD and RMSF plots depicting the dynamic behavior of AChE in complex with three selected phytochemicals and the positive control for 100 ns. RMSD plots of protein-ligand complexes with (a) quercetin, (c) biochanin A, (e) cyperotundol, and (g) carbofuran. RMSF plots for the same protein-ligand complexes with (b) quercetin, (d) biochanin A, (f) cyperotundol, and (h) carbofuran, illustrating residue-level flexibility

stable throughout the simulation time, which reveals that the protein remained stable. No significant change in the protein structure occurred during the simulation period (Fig. 4(f)).

RMSD analyses of the positive control revealed that the protein structure showed higher deviation at the initial stages of simulation. After 20 ns of the simulation, the protein reached its equilibrium state, but the deviation observed in the protein structure was high as the protein RMSD reached 22 Å in the first 20 ns of the simulation. The average RMSD of the protein structure recorded was 20.5 Å during the MD simulation. On the

other hand, the ligand also showed higher deviation as the average RMSD recorded was 10.2 Å. Both the protein and ligand showed a higher number of deviations. The average RMSD between the protein and ligand was more than 10 Å, exceeding the acceptable window of 10 Å (Fig. 4(g)). According to the RMSF analyses, the protein was found to be fluctuating at the starting region, as the residues from 80 to 100 were found to be fluctuating for more than 13 Å. Overall, other regions of the protein were found to be stable with minor fluctuations at different regions, confirming the flexibility of the target protein (Fig. 4(h)). Thus, RMSF indicates notable fluctuations were observed at loop regions. At the same time, binding site residues remained relatively stable.

The interactions between AChE and quercetin are shown as stacked bar charts normalized over a 100 ns trajectory. Interactions lasting more than 30% of the simulation time were considered. These interactions are classified into hydrophobic, ionic, and water bridges. A H-bond was formed between Asp201 and the hydroxyl group of quercetin. H-bond with Asp201 was observed for more than 200% of the simulation time (Fig. 5(a)). This could be because several H-bonds of the same subtype formed. The same residue is also used to form water-bridged contacts. For 70% of the simulation, a second hydrogen contact formed between the quercetin carboxyl group and Gln198. Furthermore, hydrophobic interactions lasting more than 30% of the simulation time were observed with Trp213 and Phe204. Water-mediated interactions with Tyr250 and Glu327 were also observed. As a result, it was found that Asp201 and Gln198 were the two critical residues in forming the AChE-quercetin complex.

The hydrogen contact was observed between the Glu327 and the hydroxyl group of biochanin A, which remained for more than 75% of the simulation time (Fig. 5(b)). Another H-bond contact between residue Gly247 and the same hydroxyl group of biochanin A was observed, which remained for more than 60% of the simulation time. A strong hydrophobic interaction with the residue His567 was observed, which retained more than 120% and the same residue was also involved in forming water-bridged interactions. Another hydrogen contact was established between the Gln198 and the carboxyl group of compounds biochanin A, which was retained for 70% of the simulation time. Hydrophobic interactions were observed with residues Trp213 and Tyr457, which lasted more than 70% of the simulation time. Water-bridged interactions were also observed with residues Ser328 and Glu454. The residues formed the H-bond Thr253 and Tyr259 with the hydroxyl group of cyperotundol (Fig. 5(c)). H-bonds with residues Thr253

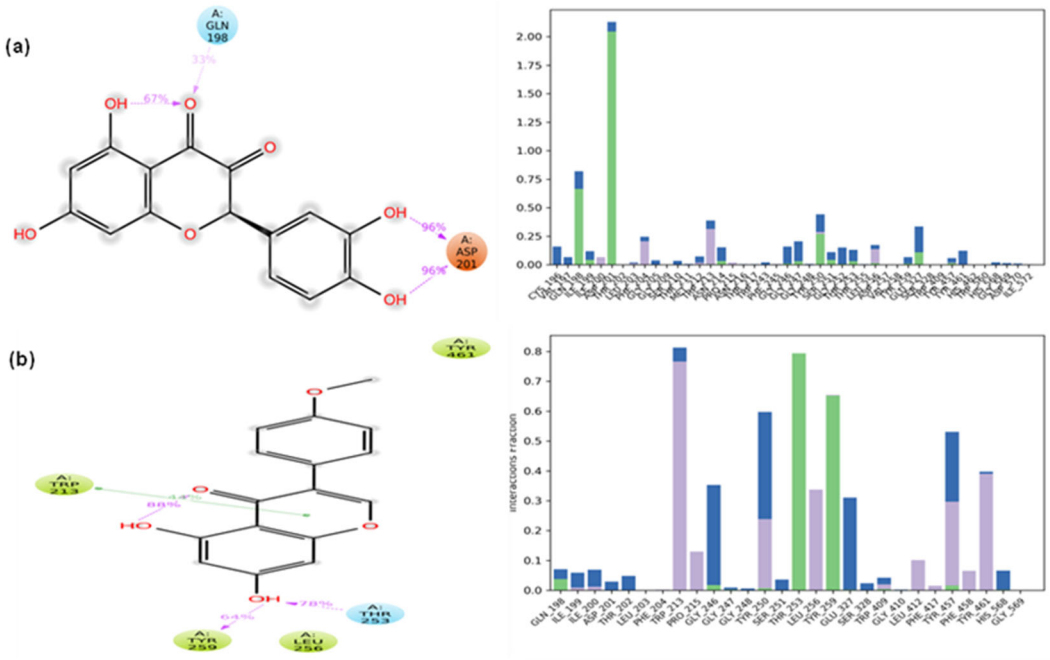

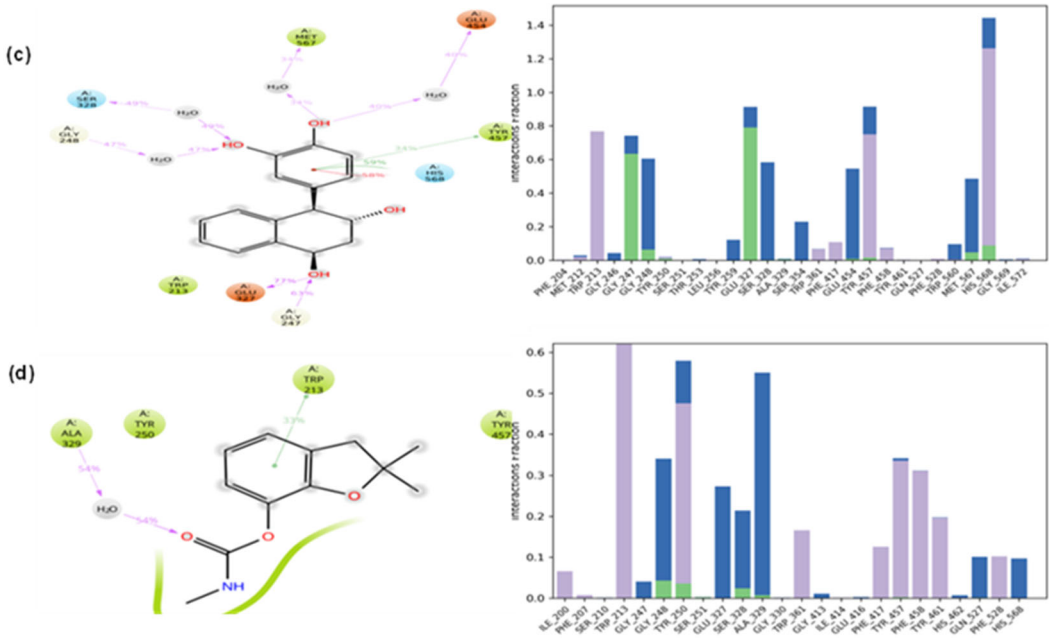

Fig 5. Schematic interaction of (a) quercetin, (b) biochanin A, (c) cyperotundol, and (d) carbofuran (control) atoms with the binding site residue of AChE

and Tyr259 was maintained for more than 70% of the simulation time. Hydrophobic interactions lasting more than 30% of the simulation time were observed with Trp213, Leu256, Tyr417, and Tyr561. Water-mediated interactions with Gly246 and Glu327 were also observed.

The interaction analysis of AChE-carbofuran showed that different amino acid residues were making H-bonds with the ligand atoms. Leu256, Tyr259, Glu327, Phe528, and His568 were found to be involved in the H-bond. The H-bonds did not last long during the MD simulation. Trp213 and His568 made a stronger bond with the ligand during different periods of the MD simulation (Fig. 5(d)). The MD simulation analyses of the three selected ligands and the positive control provided valuable insights, after observing the MD simulation results it can be seen that the three chosen ligands showed more stability than the positive control as the average RMSD and RMSF of the three selected compounds were much more reliable and less than the positive control and the interaction analyses suggested that stronger bonds were being made during the MD simulation of the three selected compounds as compared to the positive control (Fig. S1 and 5).

To determine the stability of complexes through MD simulation, the Rg of complexes was calculated (Fig. 6(a)). Compared to other receptors, the cyperotundol exhibited less variation in Rg values. The average Rg values of protein with compounds cyperotundol, biochanin A, and quercetin are 23.25, 23.52, and 23.65 Å, respectively. This small value indicates the complexes' stability. The radius of gyration of the protein complexes revealed the compactness of the protein. The three selected protein ligand complexes were similar, with time variations occurring at different time frames. Still, the protein remained, showing it was not very compact during the simulation. The Rg analyses for the positive control revealed that the protein structure's radius of gyration was much higher than the other three selected compounds, which shows that the protein did not undergo any structural changes during the MD simulation. The average Rg value for the positive control was almost 45.60, and the protein Rg went to 63.90 (Fig. 6(b)), showing significant conformational changes in the protein.

The simulated trajectories were subjected to MMGBSA binding free energy analysis to confirm the compounds' high affinity for AChE (Fig. 7). The total

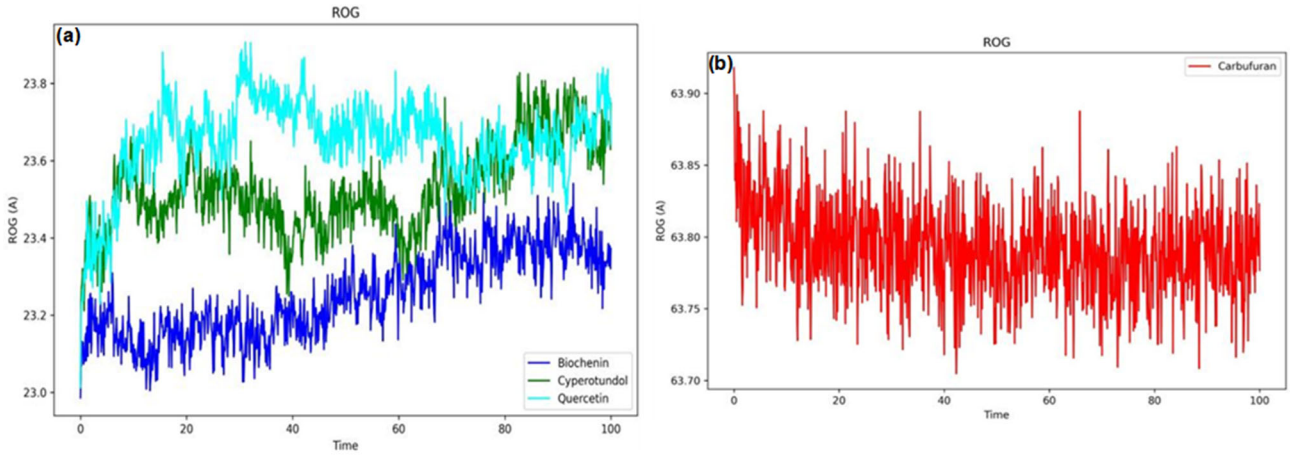

Fig 6. Rg analysis of the AChE protein receptor with (a) phytochemicals and (b) carbofuran

Table 4. MMGBSA binding free energies (kcal/mol)

Name of compound	vdW	Coulomb	Covalent	H-bond	ΔG_{total}
Carbofuran (control)	−36.84	−4.49	1.57	−0.46	−40.22
Biochanin A	−44.38	−14.8	3.17	−1.10	−57.11
Cyperotundol	−37.30	−37.25	6.63	−3.15	−71.07
Quercetin	−40.10	−28.9	4.63	−2.69	−67.06

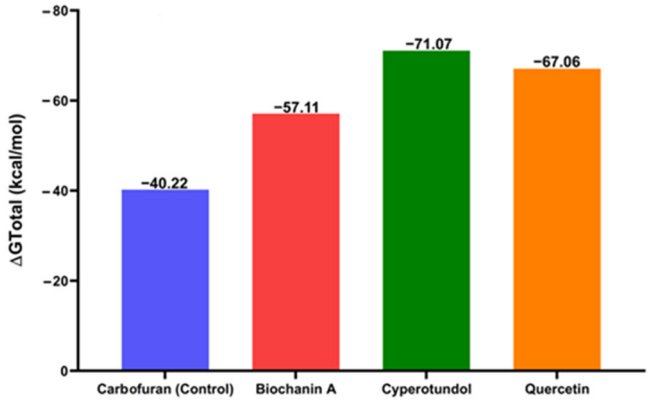

Fig 7. MMGBSA binding free energy analysis between AChE complexed with quercetin, biochanin A, cyperotundol, and carbofuran

binding energy of each complex was found to be very stable, as evidenced by the high intermolecular stability of the conformation and interaction patterns. The total binding energy of the AChE-biochanin A complex is −57.11 kcal/mol. In comparison, the net binding energy of the AChE-cyperotundol, AChE-quercetin, and AChE-carbofuran complexes is −71.07, −67.06, and −40.22 kcal/mol, respectively (Table 4). The van der Waals and Coulomb energies contributed to all complexes. The van der Waals energy to this total energy is very high compared to the Coulomb energy.

■ CONCLUSION

This study highlights the potential of *C. rotundus* phytochemicals as natural AChE inhibitors for the sustainable management of the brown planthopper (*N. lugens*). Among the nine compounds evaluated, quercetin, biochanin A, and cyperotundol demonstrated superior binding affinity and stable interactions with the AChE active site, surpassing the performance of the reference pesticide, carbofuran. Molecular docking and interaction profiling revealed that these three compounds formed stable hydrogen bonds and hydrophobic interactions critical for effective enzyme inhibition. MD simulations further confirmed these complexes' structural stability and favorable binding behavior throughout the simulation period. The pharmacokinetic and toxicity assessments indicated that the selected phytochemicals possess desirable drug-like properties, supporting their safety and efficacy. These findings suggest that quercetin, biochanin A, and cyperotundol are promising candidates for developing eco-friendly, plant-based insecticides that

offer a sustainable alternative to conventional chemical controls for brown planthopper management.

■ ACKNOWLEDGMENTS

The authors express their appreciation to Guangxi University for providing research facilities and other support.

■ CONFLICT OF INTEREST

The authors declare that they have no conflict of interest.

■ AUTHOR CONTRIBUTIONS

Saqib Hussain Bangash, Wen-Wei Tang, and Muhammad Ibrahim conceived and designed the study. Saqib Hussain Bangash, Chen-Yang Wei, and Wen-Wei Tang performed the experiments and analyzed the data. Saqib Hussain Bangash wrote the main manuscript. Saqib Hussain Bangash, Wen-Wei Tang, Amjad Hussain, Akbar Ali, Muhammad Ibrahim, and DF revised the manuscript. All the authors have read and agreed to the final version of the manuscript.

■ REFERENCES

[1] Alam, M., Lou, G., Abbas, W., Osti, R., Ahmad, A., Bista, S., Ahiakpa, J.K., and He, Y., 2024, Improving rice grain quality through ecotype breeding for enhancing food and nutritional security in Asia–Pacific region, *Rice*, 17 (1), 47.

[2] Conde, S., Catarino, S., Ferreira, S., Temudo, M.P., and Monteiro, F., 2025, Rice pests and diseases around the world: Literature-based assessment with emphasis on Africa and Asia, *Agriculture*, 15 (7), 667.

[3] Horgan, F.G., Peñalver Cruz, A., Bernal, C.C., Ramal, A.F., Almazan, M.L.P., and Wilby, A., 2018, Resistance and tolerance to the brown planthopper, *Nilaparvata lugens* (Stål), in rice infested at different growth stages across a gradient of nitrogen applications, *Field Crops Res.*, 217, 53–65.

[4] Gong, J.T., Li, Y., Li, T.P., Liang, Y., Hu, L., Zhang, D., Zhou, C.Y., Yang, C., Zhang, X., Zha, S.S., Duan, X.Z., Baton, L.A., Hong, X.Y., Hoffmann, A.A., and Xi, Z., 2020, Stable introduction of plant-virus-inhibiting *Wolbachia* into planthoppers for rice protection, *Curr. Biol.*, 30 (24), 4837–4845.e5.

[5] Liu, Z., Wu, J., Zhang, Y., Liu, F., Xu, J., and Bao, H., 2015, "Mechanisms of Rice Planthopper Resistance to Insecticides" in *Rice Planthoppers: Ecology, Management, Socioeconomics and Policy*, Eds. Heong, K.L., Cheng, J., and Escalada, M.M., Springer, Dordrecht, Netherlands 117–141.

[6] Garrood, W.T., Zimmer, C.T., Gorman, K.J., Nauen, R., Bass, C., and Davies, T.G.E., 2016, Field-evolved resistance to imidacloprid and ethiprole in populations of brown planthopper *Nilaparvata lugens* collected from across South and East Asia, *Pest. Manage. Sci.*, 72 (1), 140–149.

[7] Mota-Sanchez, D., and Wise, J., 2020, *The Arthropod Pesticide Resistance Database*, Michigan State University, http://www.pesticideresistance.org, accessed on 23 November 2023.

[8] Matsuda, K., Ihara, M., and Sattelle, D.B., 2020, Neonicotinoid insecticides: Molecular targets, resistance, and toxicity, *Annu. Rev. Pharmacol. Toxicol.*, 60, 241–255.

[9] Liao, X., Xu, P.F., Gong, P.P., Wan, H., and Li, J.H., 2021, Current susceptibilities of brown planthopper *Nilaparvata lugens* to triflumezopyrim and other frequently used insecticides in China, *Insect Sci.*, 28 (1), 115–126.

[10] Ye, W.N., Li, Y., Zhang, Y.C., Liu, Z.Y., Song, X.Y., Pei, X.G., Wu, S.F., and Gao, C.F., 2024, Area-wide survey and monitoring of insecticide resistance in the brown planthopper, *Nilaparvata lugens* (Stål), from 2020 to 2023 in China, *Pestic. Biochem. Physiol.*, 205, 106173.

[11] Khoa, D.B., Thang, B.X., Liem, N.V., Holst, N., and Kristensen, M., 2018, Variation in susceptibility of eight insecticides in the brown planthopper *Nilaparvata lugens* in three regions of Vietnam 2015–2017, *PLoS One*, 13 (10), e0204962.

[12] Datta, J., Wei, Q., Yang, Q., Wan, P.J., He, J.C., Wang, W.X., Lai, F.X., Ali, M.P., and Fu, Q., 2021, Current resistance status of the brown planthopper *Nilaparvata lugens* (Stål) to commonly used

insecticides in China and Bangladesh, *Crop Prot.*, 150, 105789.

[13] He, J., Li, B., Xie, M., Lai, F., Hu, G., and Fu, Q., 2019, Laboratory bioactivity study on neonicotinoid and other rice paddy used insecticides against the brown planthopper, *Nilaparvata lugens* (Stål) (Hemiptera: Delphacidae), *Chin. J. Rice Sci.*, 33 (5), 467–478.

[14] Cruse, C., Moural, T.W., and Zhu, F., 2023, Dynamic roles of insect carboxyl/cholinesterases in chemical adaptation, *Insects*, 14 (2), 194.

[15] Aroniadou-Anderjaska, V., Figueiredo, T.H., de Araujo Furtado, M., Pidoplichko, V.I., and Braga, M.F.M., 2023, Mechanisms of organophosphate toxicity and the role of acetylcholinesterase inhibition, *Toxics*, 11 (10), 866.

[16] Worek, F., Thiermann, H., and Wille, T., 2020, Organophosphorus compounds and oximes: A critical review, *Arch. Toxicol.*, 94 (7), 2275–2292.

[17] Rahman, M.F., Siddiqui, M.K.J., and Jamil, K., 1999, Sub-chronic effect of neem-based pesticide (Vepacide) on acetylcholinesterase and ATPases in rat, *J. Environ. Sci. Health, Part B*, 34 (5), 873–884.

[18] Bangash, S.H., Ibrahim, M., Ali, A., Wei, C.Y., Hussain, A., Riaz, M., Ur Rehman, M.F., Ahmed, F., Al-Salahi, R., and Tang, W.W., 2025, A new natural Cyperol A together with five known compounds from *Cyperus rotundus* L.: Isolation, structure elucidation, DFT analysis, insecticidal and enzyme-inhibition activities and *in silico* study, *RSC Adv.*, 15 (15), 11491–11502.

[19] Niazi, S.K., 2023, A critical analysis of the FDA's omics-driven pharmacodynamic biomarkers to establish biosimilarity, *Pharmaceuticals*, 16 (11), 1556.

[20] Weth, F.R., Hoggarth, G.B., Weth, A.F., Paterson, E., White, M.P.J., Tan, S.T., Peng, L., and Gray, C., 2024, Unlocking hidden potential: Advancements, approaches, and obstacles in repurposing drugs for cancer therapy, *Br. J. Cancer*, 130 (5), 703–715.

[21] Fu, L., Shi, S., Yi, J., Wang, N., He, Y., Wu, Z., Peng, J., Deng, Y., Wang, W., Wu, C., Lyu, A., Zeng, X., Zhao, W., Hou, T., and Cao, D., 2024, ADMETlab 3.0: An updated comprehensive online ADMET prediction platform enhanced with broader coverage, improved performance, API functionality and decision support, *Nucleic Acids Res.*, 52 (W1), W422–W431.

[22] Sun, D., Gao, W., Hu, H., and Zhou, S., 2022, Why 90% of clinical drug development fails and how to improve it?, *Acta Pharm. Sin. B*, 12 (7), 3049–3062.

[23] Gorgulla, C., 2023, Recent developments in ultralarge and structure-based virtual screening approaches, *Annu. Rev. Biomed. Data Sci.*, 6 (1), 229–258.

[24] Billones, J.B., Carrillo, M.C.O., Organo, V.G., Sy, J.B.A., Clavio, N.A.B., Macalino, S.J.Y., Emnacen, I.A., Lee, A.P., Ko, P.K.L., and Concepcion, G.P., 2017, *In silico* discovery and *in vitro* activity of inhibitors against *Mycobacterium tuberculosis* 7,8-diaminopelargonic acid synthase (*Mtb* BioA), *Drug Des., Dev. Ther.*, 11, 563–574.

[25] Yu, Y., Xu, S., He, R., and Liang, G., 2023, Application of molecular simulation methods in food science: Status and prospects, *J. Agric. Food Chem.*, 71 (6), 2684–2703.

[26] Mandlik, V., and Singh, S., 2016, Molecular docking and molecular dynamics simulation study of inositol phosphorylceramide synthase–inhibitor complex in leishmaniasis: Insight into the structure-based drug design, *F1000Research*, 5, 1610.

[27] Challapa-Mamani, M.R., Tomás-Alvarado, E., Espinoza-Baigorria, A., León-Figueroa, D.A., Sah, R., Rodriguez-Morales, A.J., and Barboza, J.J., 2023, Molecular docking and molecular dynamics simulations in relation to *Leishmania donovani*: An update and literature review, *Trop. Med. Infect. Dis.*, 8 (10), 457.

[28] Liu, J., Su, M., Liu, Z., Li, J., Li, Y., and Wang, R., 2017, Enhance the performance of current scoring functions with the aid of 3D protein-ligand interaction fingerprints, *BMC Bioinf.*, 18 (1), 343.

[29] Akhoon, B.A., Tiwari, H., and Nargotra, A., 2019, "In Silico Drug Design Methods for Drug Repurposing" in *In Silico Drug Design*, Eds. Roy, K., Academic Press, Cambridge, MA, US, 47–84.

[30] Hähnke, V.D., Kim, S., and Bolton, E.E., 2018, PubChem chemical structure standardization, *J. Cheminf.*, 10 (1), 36.

[31] Bento, A.P., Hersey, A., Félix, E., Landrum, G., Gaulton, A., Atkinson, F., Bellis, L.J., De Veij, M., and Leach, A.R., 2020, An open source chemical structure curation pipeline using RDKit, *J. Cheminf.*, 12 (1), 51.

[32] Goodsell, D.S., Sanner, M.F., Olson, A.J., and Forli, S., 2021, The AutoDock suite at 30, *Protein Sci.*, 30 (1), 31–43.

[33] Muhammed, T.M., and Aki-Yalcin, E., 2024, Molecular docking: Principles, advances, and its applications in drug discovery, *Lett. Drug Des. Discovery*, 21 (3), 480–495.

[34] Pradeepkiran, J.A., Sainath, S., Balne, P.K., and Bhaskar, M., 2021, "Computational modeling and evaluation of best potential drug targets through comparative modeling" in *Brucella Melitensis*, Academic Press, Cambridge, MA, US, 39–78.

[35] Shafqat, S., and Mahmood, T., 2023, Diversity, phylogeny and 3D protein modeling of family Acanthaceae based on RPS14 gene sequence in Pakistan, *J. Anim. Plant Sci.*, 33 (2), 397–408.

[36] Daina, A., Michielin, O., and Zoete, V., 2017, SwissADME: A free web tool to evaluate pharmacokinetics, drug-likeness and medicinal chemistry friendliness of small molecules, *Sci. Rep.*, 7 (1), 42717.

[37] Pettersen, E.F., Goddard, T.D., Huang, C.C., Couch, G.S., Greenblatt, D.M., Meng, E.C., and Ferrin, T.E., 2004, UCSF Chimera—A visualization system for exploratory research and analysis, *J. Comput. Chem.*, 25 (13), 1605–1612.

[38] BIOVIA, Dassault Systèmes, 2020, *Discovery Studio Visualizer*, Dassault Systèmes, San Diego, US.

[39] Almasabi, S.H.A., Almasoudi, H.H., Albargy, H., Alabbas, M.M.A., and Al-Mansour, F.S.H., 2025, Alternative use of droxidopa for treating cervical cancer: Inhibiting transferase, cell cycle signalling, and transport proteins via multitarget docking, DFT, MD simulations, and binding free energy studies, *Med. Oncol.*, 42 (5), 143.

[40] Mateev, E., Irfan, A., Mateeva, A., Kondeva-Burdina, M., Georgieva, M., and Zlatkov, A., 2024, *In silico* and *in vitro* screening of pyrrole-based hydrazide-hydrazones as novel acetylcholinesterase inhibitors, *Pharmacia*, 71, 1–7.

[41] Soudani, W., Hadjadj-Aoul, F.Z., Bouachrine, M., and Zaki, H., 2021, Molecular docking of potential cytotoxic alkylating carmustine derivatives 2-chloroethylnitrososulfamides analogues of 2-chloroethylnitrosoureas, *J. Biomol. Struct. Dyn.*, 39 (12), 4256–4269.

[42] Chaudhary, V., Chaturvedi, S., Wadhwa, A., Verma, P., Gautam, D., Sharma, D., Garg, A., Singh, V., Kumar, R., and Mishra, A.K., 2025, Homology modeling, molecular docking and MD simulations study of 6,7-dimethoxy-1,2,3,4-tetrahydroisoquinoline derivatives as sigma-2 receptor ligands, *J. Biomol. Struct. Dyn.*, In press, 1–15.

[43] Ali, S., Ali, U., Safi, K., Naz, F., Jan, M.I., Iqbal, Z., Ali, T., Ullah, R., and Bari, A., 2024, *In silico* homology modeling of dengue virus non-structural 4B (NS4B) protein and its molecular docking studies using triterpenoids, *BMC Infect. Dis.*, 24 (1), 688.

[44] Nhlapho, S., Nyathi, M.H.L., Ngwenya, B.L., Dube, T., Telukdarie, A., Munien, I., Vermeulen, A., and Chude-Okonkwo, U.A.K., 2024, Druggability of pharmaceutical compounds using Lipinski rules with machine learning, *Sci. Pharm.*, 3 (4), 177–192.

[45] Raghavendra, N., Kumar, B.R.P., Sasmal, P., Teli, G., Pal, R., Gurubasavaraja Swamy, P., and Sajeev Kumar, B., 2023, Designing Studies in Pharmaceutical and Medicinal Chemistry, in *The Quintessence of Basic and Clinical Research and Scientific Publishing*, Springer Nature Singapore, Singapore, 125–148.

[46] Tanchuk, V.Y., Tanin, O., Vovk, A.I., and Poda, G., 2015, A new scoring function for molecular docking based on AutoDock and AutoDock Vina, *Curr. Drug Discovery Technol.*, 12 (3), 170–178.

[47] Singh, M., Steinke, I., and Amin, R.H., 2024, Structure-based computer-aided drug design to identify potential lead molecules for asparaginyl endopeptidase inhibitors, *J. Biomol. Struct. Dyn.*, In press, 1–19.

[48] Ferreira, L.G., Dos Santos, R.N., Oliva, G., and Andricopulo, A.D., 2015, Molecular docking and structure-based drug design strategies, *Molecules*, 20 (7), 13384–13421.

[49] Hildebrand, P.W., Rose, A.S., and Tiemann, J.K., 2019, Bringing molecular dynamics simulation data into view, *Trends Biochem. Sci.*, 44 (11), 902–913.

[50] Rasheed, M.A., Iqbal, M.N., Saddick, S., Ali, I., Khan, F.S., Kanwal, S., Ahmed, D., Ibrahim, M., Afzal, U., and Awais, M., 2021, Identification of lead compounds against Scm (fms10) in *Enterococcus faecium* using computer aided drug designing, *Life*, 11 (2), 77.

[51] Choudhary, M.I., Shaikh, M., tul-Wahab, A., and ur-Rahman, A., 2020, *In silico* identification of potential inhibitors of key SARS-CoV-2 3CL hydrolase (Mpro) via molecular docking, MMGBSA predictive binding energy calculations, and molecular dynamics simulation, *PLoS One*, 15 (7), e0235030.

[52] Cordero, A.M.F., and Gonzales, A.A., 2024, Using multiscale molecular modeling to analyze possible NS2b-NS3 protease inhibitors from medicinal plants endemic to the Philippines, *Curr. Issues Mol. Biol.*, 46 (7), 7592–7618.

[53] Kandeel, M., and El-Deeb, W., 2022, Omicron variant receptor-binding domain phylogenetics and molecular dynamics, *Comput. Biol. Med.*, 146, 105633.

[54] Kikiowo, B., Oni, E.A., Iwaloye, O., Inyang, O.K., Alade, A.A., Akinwotu, S.T., and Oluwalade, O.R., 2021, Molecular interaction and inhibitory activity of dandelion's compounds on nucleoprotein: A therapeutic intervention in Lassa fever, *Biointerface Res. Appl. Chem.*, 11 (5), 12573–12583.

[55] Adasme, M.F., Linnemann, K.L., Bolz, S.N., Kaiser, F., Salentin, S., Haupt, V.J., and Schroeder, M., 2021, PLIP 2021: Expanding the scope of the protein–ligand interaction profiler to DNA and RNA, *Nucleic Acids Res.*, 49 (W1), W530–W534.

[56] Scholz, C., Knorr, S., Hamacher, K., and Schmidt, B., 2015, DOCKTITE: A highly versatile step-by-step workflow for covalent docking and virtual screening in the molecular operating environment, *J. Chem. Inf. Model.*, 55 (2), 398–406.

[57] Djinovic-Carugo, K., and Carugo, O., 2015, Missing strings of residues in protein crystal structures, *Intrinsically Disord. Proteins*, 3 (1), e1095697.

[58] Sahinidis, N.V., 2009, Optimization techniques in molecular structure and function elucidation, *Comput. Chem. Eng.*, 33 (12), 2055

[59] Colovos, C., and Yeates, T., 1993, Verification of protein structures: Patterns of nonbonded atomic interactions, *Protein Sci.*, 2 (9), 1511–1519

[60] Eisenberg, D., Lüthy, R., and Bowie, J.U., 1997, VERIFY3D: Assessment of protein models with three-dimensional profiles, *Methods Enzymol.*, 277, 396–404.

[61] Wiederstein, M., and Sippl, M.J., 2007, ProSA-web: Interactive web service for the recognition of errors in three-dimensional structures of proteins, *Nucleic Acids Res.*, 35 (Suppl. 2), W407–W410.

[62] Zhang, Y., Yang, B., Li, J., Liu, M., and Liu, Z., 2017, Point mutations in acetylcholinesterase 1 associated with chlorpyrifos resistance in the brown planthopper, *Nilaparvata lugens* Stål, *Insect Mol. Biol.*, 26 (4), 453–460.

[63] Kim, Y.H., and Lee, S.H., 2013, Which acetylcholinesterase functions as the main catalytic enzyme in the Class Insecta?, *Insect Biochem. Mol. Biol.*, 43 (1), 47–53.

[64] Herrera-Mayorga, V., Guerrero-Sánchez, J.A., Méndez-Álvarez, D., Paredes-Sánchez, F.A., Rodríguez-Duran, L.V., Niño-García, N., Paz-González, A.D., and Rivera, G., 2022, Insecticidal activity of organic extracts of *Solidago graminifolia* and its main metabolites (quercetin and chlorogenic acid) against *Spodoptera frugiperda*: An *in vitro* and *in silico* approach, *Molecules*, 27 (10), 3325.

[65] Kukreja, S., Yadav, A.K., Nehe, S., and Dharavath, S., 2024, Employing the trifluoromethyl group on a 5/5 fused triazolo[4,3-*b*][1,2,4]triazole backbone: A viable strategy for attaining balanced energetics, *Org. Lett.*, 26 (49), 10611–10615.

[66] Li, B., Chen, D., Wang, J., Yan, Z., Jiang, L., Deliang D., He, J., Luo, Z., Zhang, J., and Yuan, F., 2014, MOFzyme: Intrinsic protease-like activity of Cu-MOF, *Sci. Rep.*, 4 (1), 6759.

[67] Li, M., Gao, X., Lan, M., Liao, X., Su, F., Fan, L., Zhao, Y., Hao, X., Wu, G., and Ding, X., 2020, Inhibitory activities of flavonoids from *Eupatorium adenophorum* against acetylcholinesterase, *Pestic. Biochem. Physiol.*, 170, 104701.

[68] Yin, W., Wang, Y., Liu, L., and He, J., 2019, Biofilms: The microbial "protective clothing" in extreme environments, *Int. J. Mol. Sci.*, 20 (14), 3423.

[69] Ishaq, M., Tahira, R., Javed, A., Jamal, A., Raja, M.U., Munir, A., and ur-Rehman, A., 2017, Lemongrass essential oil as an alternate approach to manage seed associated fungi of wheat and rice, *Int. J. Agric. Biol.*, 19, 1301–1306.

[70] Nittinger, E., Inhester, T., Bietz, S., Meyder, A., Schomburg, K.T., Lange, G., Klein, R., and Rarey, M., 2017, Large-scale analysis of hydrogen bond interaction patterns in protein–ligand interfaces, *J. Med. Chem.*, 60 (10), 4245–4257.

[71] da Fonseca, A.L., Nunes, R.R., Braga, V.M.L., Comar Jr, M., Alves, R.J., de Pilla Varotti, F., and Taranto, A.G., 2016, Docking, QM/MM, and molecular dynamics simulations of the hexose transporter from *Plasmodium falciparum* (PfHT), *J. Mol. Graphics Modell.*, 66, 174–186.

[72] Heitmeier, M.R., Hresko, R.C., Edwards, R.L., Prinsen, M.J., Ilagan, M.X.G., Odom John, A.R., and Hruz, P.W., 2019, Identification of druggable small molecule antagonists of the *Plasmodium falciparum* hexose transporter PfHT and assessment of ligand access to the glucose permeation pathway via FLAG-mediated protein engineering, *PLoS One*, 14 (5), e0216457.

[73] Lipinski, C.A., 2000, Drug-like properties and the causes of poor solubility and poor permeability, *J. Pharmacol. Toxicol. Methods*, 44 (1), 235–249.

[74] Veber, D.F., Johnson, S.R., Cheng, H.Y., Smith, B.R., Ward, K.W., and Kopple, K.D., 2002, Molecular properties that influence the oral bioavailability of drug candidates, *J. Med. Chem.*, 45 (12), 2615–2623.

[75] Chang, L.C.W., Spanjersberg, R.F., von Frijtag Drabbe Künzel, J.K., Mulder-Krieger, T., van den Hout, G., Beukers, M.W., Brussee, J., and IJzerman, A.P., 2004, 2,4,6-Trisubstituted pyrimidines as a new class of selective adenosine A1 receptor antagonists, *J. Med. Chem.*, 47 (26), 6529–6540.

[76] Ertl, P., Rohde, B., and Selzer, P., 2000, Fast calculation of molecular polar surface area as a sum of fragment-based contributions and its application to the prediction of drug transport properties, *J. Med. Chem.*, 43 (20), 3714–3717.

[77] Paramashivam, S.K., Elayaperumal, K., Bhagavan Natarajan, B., Devi Ramamoorthy, M., Balasubramanian, S., and Dhiraviam, K.N., 2015, *In silico* pharmacokinetic and molecular docking studies of small molecules derived from *Indigofera aspalathoides* Vahl targeting receptor tyrosine kinases, *Bioinformation*, 11 (2), 73–84.

[78] Clark, D.E., 1999, Rapid calculation of polar molecular surface area and its application to the prediction of transport phenomena. 1. Prediction of intestinal absorption, *J. Pharm. Sci.*, 88 (8), 807–814.

[79] Variya, B.C., Modi, S.J., Savjani, J.K., and Patel, S.S., 2016, *In silico* molecular docking and pharmacokinetic prediction of gallic acid derivatives as PPAR-γ agonists, *Int. J. Pharm. Sci.*, 9 (1), 102–107.

[80] Ya'u Ibrahim, Z., Uzairu, A., Shallangwa, G., and Abechi, S., 2020, Molecular docking studies, drug-likeness and *in-silico* ADMET prediction of some novel β-amino alcohol grafted 1,4,5-trisubstituted 1,2,3-triazoles derivatives as elevators of p53 protein levels, *Sci. Afr.*, 10, e00570.